IntechOpen Journals

Green Energy and Environmental Technology

RESEARCH PAPER

Dynamic Operation Planning Model of Air-Conditioning Based on Weather Forecast: Heat Resource Usage Considering Energy Saving and Room Comfort

Ichito Miyajima, Kaoru Kuramoto and Satoshi Kumagai*

Department of Industrial and System Engineering, Aoyama Gakuin University, Japan
*Corresponding author. E-mail: kumagai@ise.aoyama.ac.jp

Abstract

Air-conditioning systems must save energy while maintaining an appropriate room environment. In heat management, there is a tradeoff between the requirement to save energy during heat production and individual heat consumption for maintaining comfort. Heat consumption is dependent on environmental conditions in a given room, including the thermal load of the room and ambient weather. To predict thermal load, regression models can be built using weather forecast data, and the heat level necessary to avoid heat stroke while maintaining comfort can be calculated. In this study, we propose a decision-making process model of heat resource allocation for facility managers, known as a dynamic air-conditioning operation plan. The heat level allocated may change, considering the gap between planned and actual heat usage on a daily and monthly basis, and the resource is then distributed according to the thermal load. If the actual heat usage is expected to exceed the monthly target by the middle of the month, the plan is then revised to use the heat resource allocated for the following month, ahead of schedule. To demonstrate effectiveness of the model, sensitivity analysis was performed based on measured data.

Keywords: building energy management system, heat resource allocation, resource storing, energy saving

Citation
Ichito Miyajima, Kaoru Kuramoto and Satoshi Kumagai (2023), Dynamic Operation Planning Model of Air-Conditioning Based on Weather Forecast: Heat Resource Usage Considering Energy Saving and Room Comfort. *Green Energy and Environmental Technology* 2(1), 1–26.

DOI
https://doi.org/10.5772/geet.22

Received: 16 June 2023
Accepted: 29 November 2023
Published: 28 December 2023

1. Introduction

Building and Energy Management Systems (BEMS) are commonly used for air-conditioning [1–3]. BEMS monitors and controls the energy requirements of an entire building, ensuring demand control during peak power consumption. Peak cut control is a feature that temporarily limits power supply when consumption exceeds the contracted amount. However, room comfort may decrease during peak cuts, increasing the risk of heatstroke. Predicting daily thermal resource consumption, understanding the differences in actual consumption, and conducting proper air-conditioning operations are, therefore, crucial.

Heat resource consumption is influenced by various factors such as weather, building structure, room characteristics, location, orientation, and more. Several studies have estimated energy consumption at the building or subcomponent level [4]. For example, Tanaka et al. [5] estimated annual energy consumption from air-conditioning and hot water systems using actual data. Agarwal *et al.* [6] analysed energy consumption for campus buildings using data collected from BEMS. Rice *et al.* [7] provided a model for estimating energy consumed during heating, ventilation, and air conditioning systems in buildings. These studies estimate medium to long-term energy consumption for entire buildings.

Facility managers implement daily energy-saving actions based on building thermal loads and consumption. Therefore, predicting daily thermal loads is necessary. Various methods, including Kalman filters [8], linear regression models [9], time series models and neural networks [10], have been proposed for thermal load prediction. All these methods require past thermal load training data.

Previous studies on optimizing heat resource operations based on thermal load prediction have demonstrated efficient operational methods for facility managers and heat providers [11–14]. Fei Wang *et al.* [15] proposed a multi-objective planning method considering the comfort of individual rooms in thermal resource supply. This model assumes that the thermal characteristics of individual rooms are the same. Kumagai *et al.* [16] proposed operational methods for air-conditioning system based on different thermal characteristics for each room, considering thermal inertia of rooms.

The thermal characteristics of individual rooms depend on various factors [17], including building structure, orientation, room usage, heat-generating equipment, neighbouring room influences, heat radiation from windows and walls, and room heat storage capacity. Additionally, meteorological conditions such as outside temperature, humidity, and sunlight affect daily room heat consumption prediction accuracy of weather forecasts [18]. Accuracy decreases for medium and long-term forecasts compared to short-term ones. Furthermore, maintaining accuracy in thermal load prediction using past training data becomes challenging as the forecast horizon extends.

Predicted and actual heat consumption may vary. If room comfort goals cannot be achieved within the available heat resource range, facility managers may need to adjust temperature settings or reduce available heat resources. Extending the planning period to achieve the target heat consumption may also be necessary. This study models the decision-making process for facility managers' daily, monthly, and annual heat resource allocation plans and proposes dynamic air-conditioning operation plans based on heat resource demand forecasts, considering weather forecasts.

Room-specific heat consumption is predicted for ten days in advance using regression models that account for weather conditions. Based on predicted heat consumption, daily planned heat resource is allocated to rooms. The difference between daily planned heat consumption and actual daily heat consumption is considered to adjust the target heat consumption. Daily heat distribution based on individual room characteristics is also carried out. Additionally, heat distribution amounts are modified considering room environment, actual heat consumption, and planning period. For example, if it becomes apparent that monthly actual heat consumption will exceed the monthly target heat consumption midway through the month, adjustments may be made, such as utilizing next month's target thermal resources in advance.

2. *Materials and methods*

2.1. Design process of the air-conditioning operations

Energy-saving actions or strategies must consider the cooling of the building on a room-by-room basis, while maintaining comfort and safety. The heat resource consumption of each room is dependent on the ambient weather conditions and room environment to be achieved. If the air-conditioning requirements are entrusted to the occupants of the individual rooms in a building, they would have the freedom and flexibility to achieve the ambient comfort they prefer. This creates difficulty in achieving energy-saving targets.

In addition to the inaccuracy of weather forecasts, the differences in room usage conditions make it difficult to predict the thermal loads. The operating status of heat sources, including occupants and computers in the room, also has a significant impact on heat consumption. There is always a discrepancy between the target value and actual value of heat consumption.

The facility manager is expected to implement the plan-do-check-act/adjust (PDCA) process to manage the heat consumption target. In dynamic air-conditioning operation plan, the target amount of heat consumed could change depending on the gap between planned and actual use of heat resources on a daily basis, and the daily amount of heat resources could be distributed according to the predicted thermal load of each room.

Following this, a regression model is used for estimating the room environment when the air-conditioning starts operating using weather forecasts. The daily thermal load of the room is calculated based on the difference between room environments at the start-up and target.

The dynamic air-conditioning operation planning model is proposed. If the actual heat use is expected to exceed the monthly target by the middle of the month, the plan could then be revised to use the heat resource allocated for the next month, ahead of schedule. The model enables the indoor environment to be maintained even if the weather forecast accuracy fluctuates and the planned heat consumption differs from the actual heat consumption. To demonstrate the effectiveness of the model, a sensitivity analysis is performed based on the accuracy of the weather forecast, and subsequent effects are analysed.

2.2. Forecasting room environment using weather forecast

Based on weather forecast data, the initial room environment prediction model predicted the room environment before air-conditioning began, i.e., the initial state of the room environment, which was described using the discomfort index (DI) and heat index when the air-conditioning operation began. Additionally, the initial state of the room was predicted after a sufficient amount of time had passed since the previous air-conditioning operation, and it is assumed that the amount of heat input until the previous day was not retained in the room.

DI quantitatively expresses the heat and humidity of summer [19], and is calculated using Equation (1) based on the temperature t_p (°C) and humidity h (%) data:

$$\mathrm{DI} = 0.81t_p + 0.01h(0.99t_p - 14.3) + 46.3. \tag{1}$$

For example, the DI was 75 at 27 °C and 55% humidity, but it was 80 at 29 °C and 70% humidity. When the DI exceeds 75, 10% of the population becomes uncomfortable, but when it exceeds 80, the entire population becomes uncomfortable. In Japan, some people start feeling uncomfortable when the DI reaches 77, and 93% of the population feels uncomfortable when the DI reaches 85.

Wet-bulb globe temperature (WBGT) is a heat index that expresses the risk of exposing a room occupant to excessive heat [20]. WBGT is related to five factors; temperature, relative humidity, wind speed, radiant heat, and workload.

WBGT can be calculated through two methods using Equations (2) and (3), depending on the solar radiation conditions. The dry-bulb and wet-bulb temperatures are the temperatures at which the dry-bulb and wet-bulb of the psychrometer are read, respectively. Relative humidity can be calculated based on the difference between dry-bulb and wet-bulb temperatures. The black bulb thermometer measures the black globe temperature and effect of the radiant heat.

In this study, Equation (3) was used when the solar radiation effect was negligible, for example, when indoors. Therefore, WBGT was calculated using Equation (3).

With the effect of sunlight, for example, when outdoors, WBGT is calculated as follows:

$$WBGT = 0.7Wbt + 0.2Bbt + 0.1Dbt \tag{2}$$

where,

Wbt: Wet bulb temperature (°C)

Bbt: Black bulb temperature (°C)

Dbt: Dry bulb temperature (°C).

When the effect of sunlight can be neglected, for example, when indoors, WBGT is calculated as follows:

$$WBGT = 0.7Wbt + 0.3Dbt. \tag{3}$$

If the WBGT value is <25 °C, the risk of heat stroke is minimal; however, if it is ≥25 °C, the risk of heat stroke must be closely monitored, but if it is ≥28 °C, the risk of heat stroke is significant.

2.3. Forecasting the environment evaluation index

In this study, the initial value of the room environment was predicted based on the weather forecast from Day 1–10. For example, if the plan was designed on June 1, the forecast target will be from June 2 to June 11, whereas if the plan is designed on June 2, a day after the previous plan was designed, the forecast target will be from June 3 to June 12. In this case, forecasts were duplicated for 9 d, i.e., June 3–June 11. The plan is based on the forecast results as of June 2 to allow revision of the plan according to more probable forecasts each time. Table 1 shows the referenced weather forecast parameters.

Table 1. Weather forecast parameters.

Parameters	Detail
Highest temperature	Unit: °C; Value in 1 °C
Lowest temperature	Unit: °C; Value in 1 °C
Precipitation	Unit: %; Value in 5%
Precipitation amount	Unit: mm; Value in 0.01 mm
Lightning probability	Unit: %; Value in 1%
Wind speed	Unit: m/s; Value in 0.1 m/s
Sunlight rate	Unit: %; Value in 1%
Daylight hours	Unit: hour; Value in 0.1 h
Minimum humidity	Unit: %; Value in 1%

The initial state of the room, before initiating the air-conditioning operation, depends on external weather conditions and can be expressed using Equations (4) and (5) based on the weather forecast parameters shown in Table 1. In this model, the target forecast date is forecast time t', and the collection date for the weather forecast data is the observation time t. For example, if the initial value of the living environment is predicted on June 3 as of June 1, t' = June 3 and t = June 1.

Equations (4) and (5) indicate the regression models using the DI or heat index at 9:00 am in the room as objective variables, and maximum and minimum temperature, precipitation probability, precipitation, lightning probability, wind speed, sunshine rate, sunshine duration, and minimum humidity as explanatory variables.

$$D^{t'} = \sum_{k=1}^{k=9} a_k x_k^t + a_0 \tag{4}$$

where,

$D^{t'}$: Initial value of the discomfort index

a_i: Partial regression coefficient

x_1^t: Maximum temperature

x_2^t: Minimum temperature

x_3^t: Precipitation probability

x_4^t: Precipitation

x_5^t: Lightning probability

x_6^t: Wind speed

x_7^t: Sunshine rate

x_8^t: Sunshine duration

x_9^t: Minimum humidity

t': Forecast time

t: Observation time.

$$W^{t'} = \sum_{k=1}^{k=9} b_k x_k^t + b_0 \tag{5}$$

where,

$W^{t'}$: Intial value of WBGT

b_0: Intercept

b_k: Partial regression coefficient.

Tables 2–7 demonstrate the regression analysis results of the DI and WBGT. The contribution rates and F-values indicate that both the DI and WBGT are statistically significant. Furthermore, based on the analysis results for each explanatory variable, the degree of influence on the prediction can be understood by comparing corresponding P-values. The minimum temperature, sunshine rate, and amount of sunshine showed a significantly large influence, while minimum humidity and precipitation probability showed marginal influence.

The regression model of the DI in the rooms' initial state showed a contribution rate of R^2 = 0.894. The partial correlation coefficient/estimate error of the partial correlation coefficient assumedly followed the t distribution. Based on the P-value (Table 4), the null hypothesis, which stated that the partial regression coefficient is

Table 2. Regression statistics (Discomfort index, DI).

Multiple correlation R	0.946
Multiple coefficient of determination R^2	0.894
Adjusted R^2	0.888
Standard error	1.038
Sample size	170

Table 3. Scatter analysis (DI).

	Degree of freedom	Fluctuation	Variance	Observed variance ratio	Significance (F)
Regression	9	1460.60	162.28	150.51	2.36E-73
Residual	160	172.511	1.078	–	–
Total	169	1633.11	–	–	–

Table 4. Regression line coefficient (DI).

Partial regression coefficient		Standard error	P-value
a_0	8.314	0.924	6.2322E-16
a_1	0.208	0.055	0.0002289
a_2	0.503	0.056	1.1157E-15
a_3	0.008	0.007	0.30157765
a_4	0.021	0.011	0.05764161
a_5	−0.013	0.008	0.10535958
a_6	−0.080	0.079	0.31597638
a_7	0.127	0.020	8.6137E-10
a_8	−0.887	0.146	7.8887E-09
a_9	−0.006	0.011	0.58420124

Table 5. Regression statistics (Wet-bulb globe temperature, WBGT).

Multiple correlation R	0.953
Multiple coefficient of determination R^2	0.909
Adjusted R^2	0.904
Standard error	1.351
Sample size	170

Table 6. Scatter analysis (WBGT).

	Degree of freedom	Fluctuation	Variance	Observed variance ratio	Significance F
Regression	9	2916.8	324.0	177.62	1.62E-78
Residual	160	291.9	1.824	–	–
Total	169	3208.7	–	–	–

Table 7. Regression line coefficient (WBGT).

Partial regression coefficient		Standard error	P-value
b_0	55.81	1.20	8.8445E-95
b_1	0.300	0.072	4.535E-05
b_2	0.703	0.073	2.038E-17
b_3	0.012	0.010	0.20507361
b_4	0.034	0.015	0.02060772
b_5	−0.016	0.011	0.13583822
b_6	−0.155	0.103	0.13533141
b_7	0.220	0.025	4.7013E-15
b_8	−1.523	0.189	1.898E-13
b_9	−0.019	0.015	0.21335469

zero, is rejected. Therefore, the DI of the initial state of the living room is fully explained by the linear combination of the maximum and minimum temperature, precipitation probability and amount, lightning probability, wind speed, sunshine rate and duration, and minimum humidity. Therefore, the regression model of the DI is suitable.

The regression model for the WBGT in the initial state of the room showed a contribution rate of R^2 = 0.999. The partial correlation coefficient/estimate error of the partial correlation coefficient assumedly followed the t distribution. The P-value in Table 7 indicate that the null hypothesis, which stated that the partial regression coefficient is zero, is rejected. Therefore, WBGT in the initial state of the room was completely explained by the linear combination of the maximum and minimum temperature, precipitation probability and amount, lightning probability, wind speed, sunshine rate and duration, and minimum humidity. Therefore, the regression model of WBGT is suitable.

3. Dynamic air-conditioning operation planning model

Figure 1 shows the outline of the dynamic air-conditioning operation planning model. The procedure of the model can be described by the following steps:

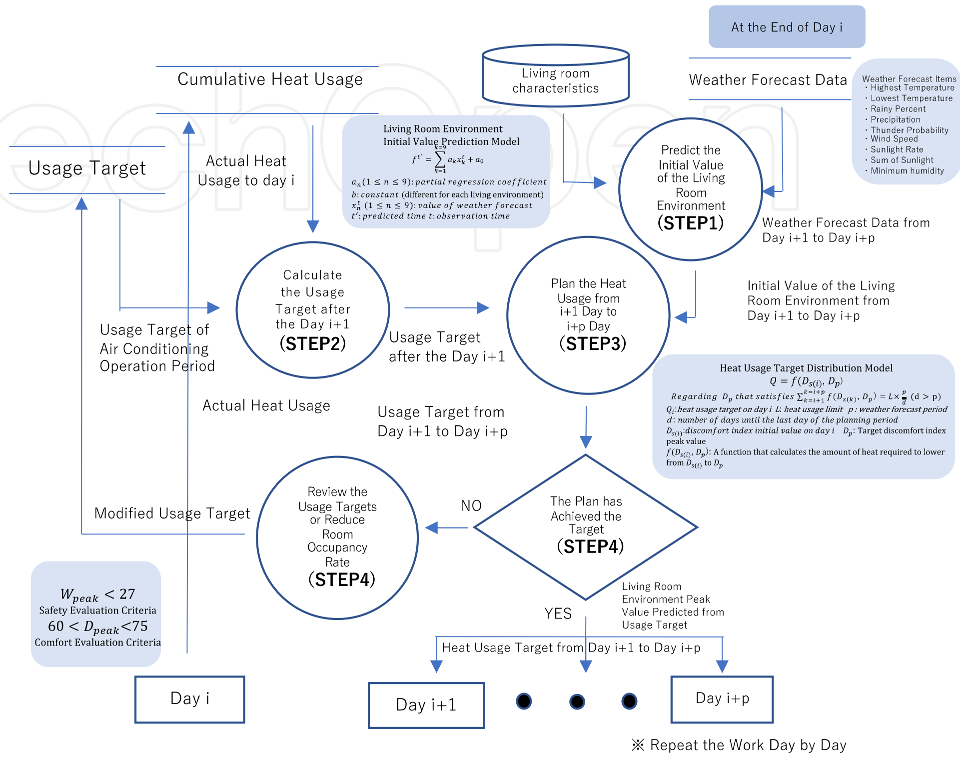

Figure 1. Process flowchart of the dynamic air-conditioning operation planning model.

Step 1: The initial values of the DI and WBGT of the room environment are predicted using Equations (4) and (5) based on the weather forecast data. Initial values are measured before the air-conditioning system commences operation in the room. These values are dependent not only on the weather forecast data but also on the thermal characteristics of the room, and include direction, volume, thermal insulation performance, heat generation equipment, and the number of residents in the room.

Step 2: The amount of heat resource that can be used in future cooling operations is obtained by subtracting the cumulative amount of actual heat resources used from the target heat resource. The cumulative amount of heat resource used refers to the actual amount of heat consumed to that level. The target amount of heat resource refers to the amount of heat resource that can be used while planning and decreases gradually.

Step 3: Based on available heat resources calculated in Step 2, and the initial DI and WBGT values calculated in Step 1, the heat consumption target is allocated daily.

Step 4: Whether the target room environment can be realized by the amount of distributed heat resources is checked. If it cannot be estimated then the monthly target heat resource is increased, room occupancy rate is suppressed, or the plan is revised using the target usable heat resources allocated for the next month. Thus, bias from the weather, such that a hot or comfortable week appears more than the usual frequency, is addressed, and a sudden change in the living room environment is suppressed.

3.1. Heat resource consumption necessary to prevent heat stroke risk and maintain comfort

By repeating these steps daily, the target amount of heat resources used changes according to the gap between planned and actual utilization of the heat resource, and the daily amount of heat resources is allocated according to the thermal load of each room. If the actual heat resource consumption is expected to exceed the monthly target heat resources, then the plan can be revised to use the heat resources allocated for the next month in advance.

The amount of heat required to transition to the target value of the room environment can be predicted by its initial and target values. The heat demand can be expressed by the amount of heat used at the start-up operation and the amount of heat used during the continuous operation using Equation (6):

$$q_i = u_{su} + u_c \tag{6}$$

where,

q_i: predicted heat usage on the ith day (J)

u_{su}: predicted heat usage at the start-up time operation (J)

u_c: predicted heat usage at continuous operation (J).

The start-up operation is the phase during which heat is supplied for a short duration from the beginning of the operation, when the air-conditioning fan is switched on, until the room temperature reaches the desired temperature. During this continuous operation, heat is continuously supplied until the end of the operation to maintain the desired temperature.

The predicted heat consumption at the start-up operation was calculated using Equation (7). The amount of heat per hour at the start-up operation, $u_{su,\,ps}\,(D_{s\,(i)}, D_p)$, is a constant that is determined by the difference between the current and target values and the room characteristics. The time required for the start-up operation, T_{su}, is a constant that is determined by the fan coil unit (FCU) capacity of the room.

The predicted heat consumption per hour during continuous operation is calculated using Equation (8). It is proportional to the constant determined by the difference between the current and target values, $u_{c,\,ps\,(D_{s\,(i)},\,D_p)}$, operating time, $\{(t_e - t_s) - T_{su}\}$, and room characteristics.

To ensure comfort, it is essential to prioritize appropriate discomfort index targets. Operations based on WBGT targets should be restricted to times with a low risk of heatstroke.

$$u_{su} = u_{su,ps(D_{s(i)},D_p)} T_{su} \tag{7}$$

$$u_c = u_{c,ps(D_{s(i)},D_p)} \{(t_e - t_s) - T_{su}\} \tag{8}$$

where,

$u_{su,\,ps\,(D_{s\,(i)},\,D_p)}$: Heat consumption required per hour during the start-up operation to change the DI from $D_{s\,(i)}$ to D_p (kJ/s)

T_{su}: Start-up operation time (s)

$u_{c,\,ps\,(D_{s\,(i)},\,D_p)}$: Heat consumption required per hour during the continuous operation, to change the DI from $D_{s\,(i)}$ to D_p (kJ/s)

t_s: Start time of the operation (hh:mm:ss)

t_e: End time of the operation (hh:mm:ss)

$D_{s\,(i)}$: Initial value of the DI on the ith day

D_p: Target peak value of the DI.

Equations (9) and (10) indicate the amount of heat required for the start-up and continuous operations when the room environment is expressed by WBGT:

$$u_{su} = u_{su,ps(W_{s(i)},W_p)} T_{su} \tag{9}$$

$$u_c = u_{c,ps(W_{s(i)},W_p)} \{(t_e - t_s) - T_{su}\} \tag{10}$$

where,

$W_{s\,(i)}$: Initial value of WBGT on the ith day

W_p: Target peak value of WBGT.

3.2. Heat allocation method

Based on the initial value of the room environment (Equations (4) and (5)), heat resource was allocated to the room within range of the available resources through its efficient use to improve and stabilize the comfort of the room, which does not fluctuate daily. This means that during the weather forecast period, the target room comfort was constant based on the weather forecast, and room comfort was pursued within range of usable heat.

Based on the initial values of the room environment for the following few days predicted using Equations (4) and (5) and the amount of heat that can be used on a working day, the feasible room environment after the air-conditioning operation was calculated. The amount of heat required to achieve the room environment was calculated daily for several days and was used as the amount of heat utilized. When the DI is used as the evaluation index, the amount of heat required for each day can be expressed as Equations (11), (12), (13), and (14). Equation (14) is obtained using Equations (7) and (8).

$$\sum_{k=i+1}^{k=i+p} f^{Q}(D_{s(k)}, D_p) = \frac{Lp}{d}(d > p) \tag{11}$$

$$\sum_{k=i+1}^{k=i+p} f^{Q}(D_{s(k)}, D_p) = L(d \leq p). \tag{12}$$

The target peak value of the DI (D_p) that satisfies Equations (11) or (12) was calculated using Equation (13):

$$Q_i = f^{Q}(D_{s(i)}, D_p) \tag{13}$$

$$f^{Q}(D_{s(i)}, D_p) = u_{su,ps(D_s(i),D_p)} T_{su} + u_{c,ps(D_s(i),D_p)} \{(t_e - t_s) - T_{su}\} \tag{14}$$

where,

Q_i: Heat amount used on the ith day

L: Usable heat amount (J)

p: Prediction period

d: Number of days remaining until the last day of the operation period (d)

$f^{Q}(D_{s\,(i)}, D_p)$: The amount of heat required to reduce the discomfort index from $D_{s\,(i)}$ to D_p (J).

When WBGT was used as the evaluation index, the amount of heat required for each day is expressed using Equations (15), (16), (17), and (18). Equation (18) was obtained from Equations (9) and (10).

$$\sum_{k=i+1}^{k=i+p} f^{Q}(W_{s(k)}, W_p) = \frac{Lp}{d}(d > p) \tag{15}$$

$$\sum_{k=i+1}^{k=i+p} f^{Q}(W_{s(k)}, W_p) = L(d \leq p). \tag{16}$$

Target peak value of WGBT, W_p, which satisfies Equations (15) or (16), was calculated using Equation (17).

$$Q_i = G^{Q}(W_{s(i)}, W_p) \tag{17}$$

$$G^{Q}(W_s(i), W_p) = u_{su,ps(W_s(i),W_p)} T_{su} + u_{c,ps(W_{s(i)},W_p)}\{(t_e - t_s) - T_{su}\} \tag{18}$$

where,

$G^{Q}(W_{s\,(i)}, W_p)$: Amount of heat required to reduce WBGT from $W_{s\,(i)}$ to W_p (J).

4. Model verification

4.1. Stability of heat resource allocation

To demonstrate the effectiveness of the dynamic air-conditioning operation planning model, a simulation was performed based on measurement data from the 4th floor of Building O, Sagamihara Campus, Aoyama Gakuin University. This building has a water circulation-type air-conditioning system with a centralized heat source. The heat source and temperature of each room are under the centralized control of the BEMS. Further, the heat source and FCU of each room are connected by a feed-to-return water circulation-piping route to supply heat to each room. Heat is supplied to the common area through the air handling and ventilation unit. Table 8 shows the area of the living room and number of FCUs.

Table 8. Floor specifications.

Name	Floor space	Number of FCU
SR1	38.88 (40.55) m^2	2
SR2	38.88 (40.55) m^2	2
LR	116.64 (118.21) m^2	6
Total floor area	2,178 m^2	–

( ): wall included.

The environment evaluation index was set as the DI, and the heat resource was distributed according to the dynamic air-conditioning operation planning model. The amount of heat distributed was determined on the day before the air-conditioning operation commenced.

The cooling operation period was set to 4 months, from July to October (1 month was defined as 28 d), and serial numbers were assigned to each day from July 1. The transition of the air-conditioning operation and DI during this period was simulated. The weather forecast, from Day 1 to 10, was expressed as Equation (19). The prediction error assumedly followed the normal distribution of mean and standard deviation, as shown in Table 9.

$$D_r(i) = D_a(i) + \varepsilon \tag{19}$$

where,

$D_r(i)$: Simulated value of the DI on the ith day

$D_a(i)$: Actual value of the DI on the ith day

ε: Forecast error.

Operation was evaluated in terms of stability of the heat distribution without extra heat resources. When the usable heat resource was utilized, the DI in the initial state was at peak level.

4.2. Verification of the forecast model

To demonstrate the prediction efficiency of the initial value for the room environment, based on measured values of the DI and WBGT from May 1, 2020, to October 30, 2020, the difference from the value predicted 1–10 d before was calculated as the forecast error (Tables 9 and 10).

Table 9. Forecast error for each forecast date (DI).

Forecast days	Mean (%)	Standard deviation (%)
1 day ago	−0.0353	1.26
2 days ago	−0.0570	1.58
3 days ago	1.40	1.86
4 days ago	1.45	1.85
5 days ago	1.43	1.84
6 days ago	1.36	1.77
7 days ago	1.37	1.61
8 days ago	1.40	1.77
9 days ago	1.38	1.85
10 days ago	1.42	1.83

Table 10. Forecast error for each forecast date (WBGT).

Forecast days	Mean (°C)	Standard deviation (°C)
1 day ago	−0.000000476	1.01
2 days ago	−0.00180	1.11
3 days ago	0.911	1.28
4 days ago	0.938	1.27
5 days ago	0.924	1.28
6 days ago	0.877	1.23
7 days ago	0.880	1.09
8 days ago	0.895	1.09
9 days ago	0.892	1.26
10 days ago	0.905	1.24

4.3. Verification results

We examined six patterns with varying peak DI targets, WBGT targets, and available amounts of the heat resource. The DI and WBGT at 9:00 AM from July 1, 2020, to October 28, 2020, were used as the initial values of the room environment. Table 11 shows the verification conditions for the six patterns.

Table 11. Verification conditions.

	Peak discomfort index target (%)	Peak WBGT target (°C)	Amount of the usable heat (J)
Pattern 1	75	27	1,000,000
Pattern 2	75	27	1,200,000
Pattern 3	75	27	1,500,000
Pattern 4	70	25	1,000,000
Pattern 5	70	25	1,200,000
Pattern 6	75	27	1,000,000–1,200,000 (Varies monthly)

Figure 2 shows changes in the peak DI when its target was set to 75%, and the transition of WBGT during peak hours is shown when its target was set to 27 °C. Figure 3 shows the results of the peak DI target at 70%, and the transition of WBGT during peak hours is shown when its target was set to 25 °C. The initial state of the room fluctuated according to weather changes, but even if the peak DI target shifted to a comfortable level (75%–70%), a proper heat supply was achieved, and the DI was maintained at <70%. The peak WBGT target was also maintained below the heat stroke alert level. Overall, an appropriate heat supply was possible when the initial state of the room changed due to daily changes in the weather.

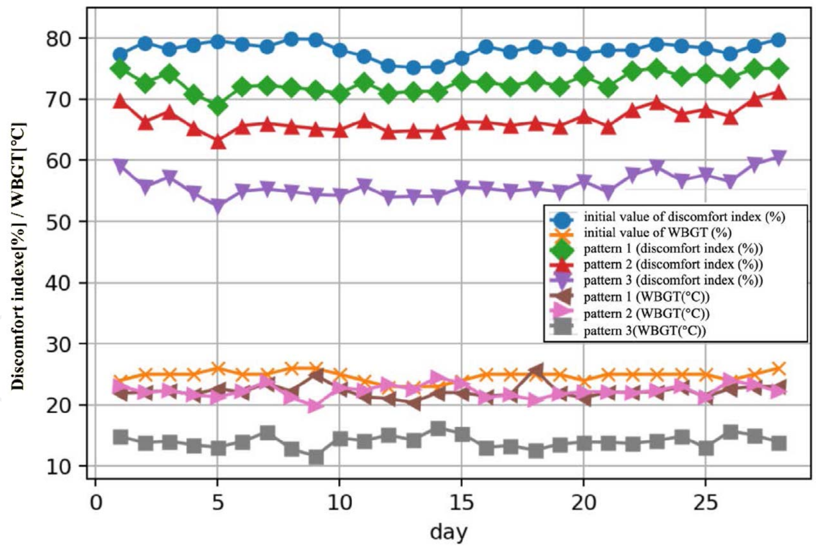

Figure 2. Results of Patterns 1, 2, and 3 (July).

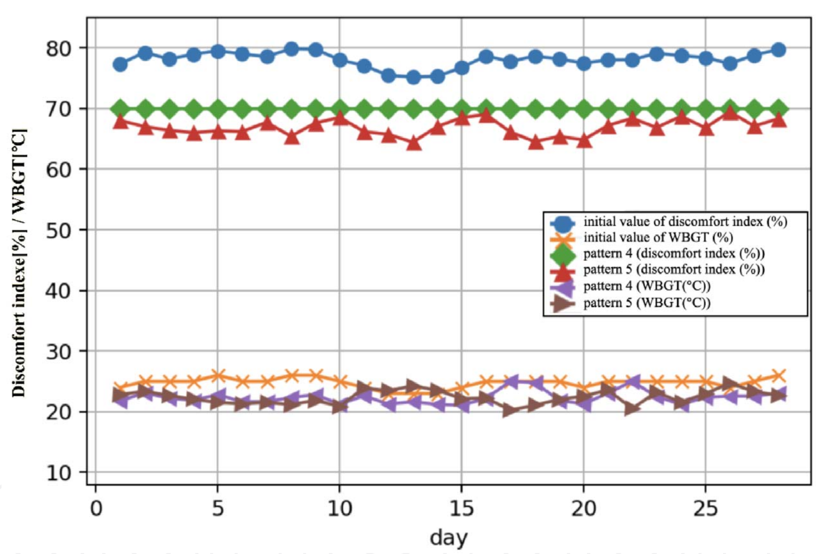

Figure 3. Results of Patterns 4 and 5 (July).

In July (Figures 2 and 3), the amount of the distributed heat resource was not sufficient to achieve the target, therefore, heat was distributed to prioritize the achievement of the target rather than for energy-saving.

Both the DI and WBGT increased in the initial state of the room as August progressed (Figure 5), but their peaks were suppressed and stable. The dynamic operation planning model responded to weather changes during this month.

If the operation period was extended to include August, a large heat resource shortage was expected. Therefore, as the initial levels of the room environment in August are higher than that in July, it is desirable to operate while preserving the heat resources.

Figure 5 shows the DI and WBGT results when the available heat resource was 20% higher in August compared to that in July. In the latter half of August, the initial values of DI and WBGT increased. However, due to the planned extension in the dynamic operation planning model, the available heat resource for the next month could be used in advance to achieve the target.

In September (Figure 6), the available heat resource was the same as that in August, however, in the latter half of the month, both initial values of the DI and WBGT decreased. Although the usable amount of heat was tight, DI at peak was at an undesired level, and WBGT exceeded the heat stroke warning level.

Figures 4–7 shows the verification results from the peak DI target set to 75%, and the amount of heat used changed monthly (Table 11, Pattern 6). Moreover, the transition of WBGT during peak hours is shown when its target during peak hours was set to 27 °C. When the amount of available heat resource changes monthly, an appropriate amount of heat should be set according to the initial value of the DI and peak DI target.

In the case of Pattern 6, surplus heat resources were available that could be used in September and October, and the need for the air-conditioning operation was

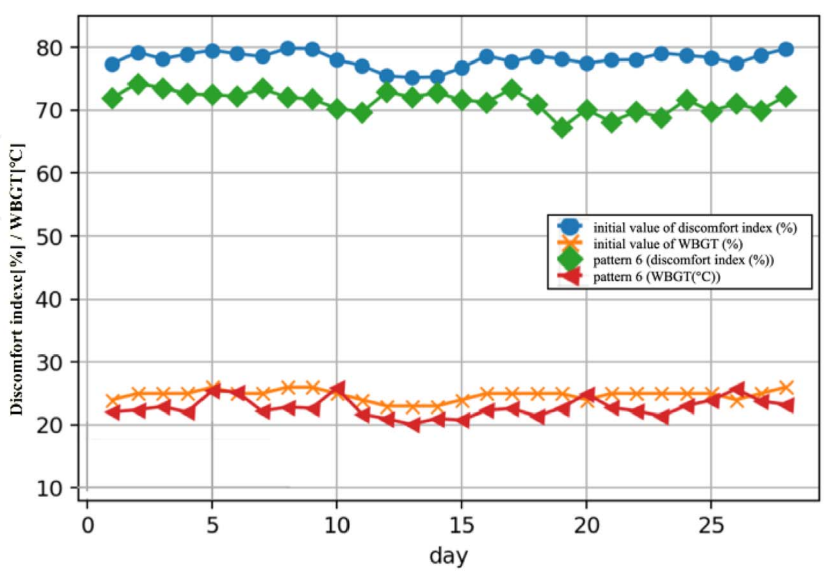

Figure 4. Results of Pattern 6 (July, Usable heat: 1,000,000 J).

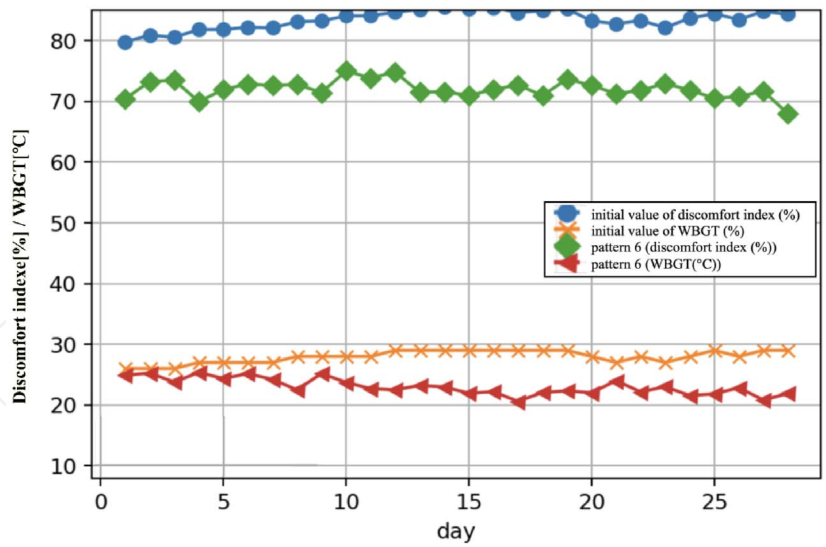

Figure 5. Result of Pattern 6 (August, Usable heat: 1,200,000 J).

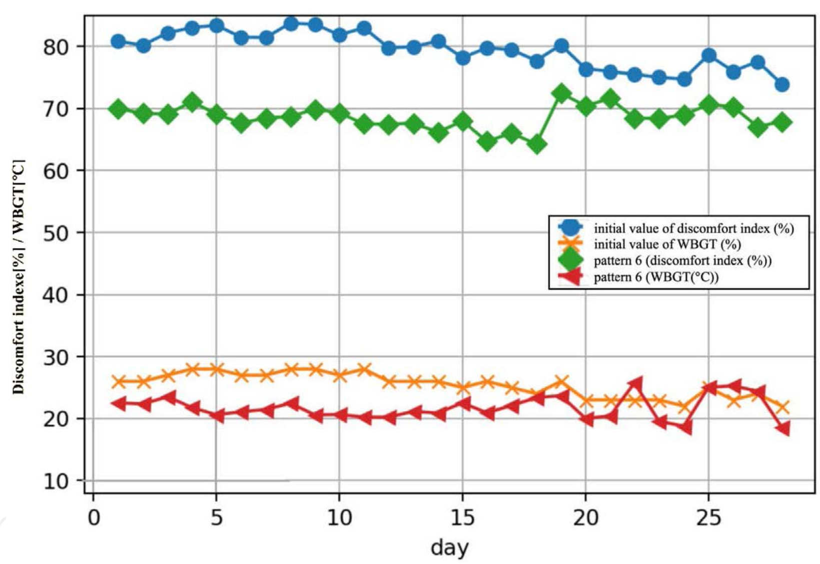

Figure 6. Results of Pattern 6 (September, Usable heat: 1,200,000 J).

particularly low in October. Therefore, if the heat demand for the next few weeks could be estimated, the surplus could then be allocated when the heat demand is high through the planned extension.

4.4. Sensitivity analysis for the accuracy of the weather forecast

The weather forecast data used in this study were affected by various factors, such as the distance from the forecast point to the measurement point, regional

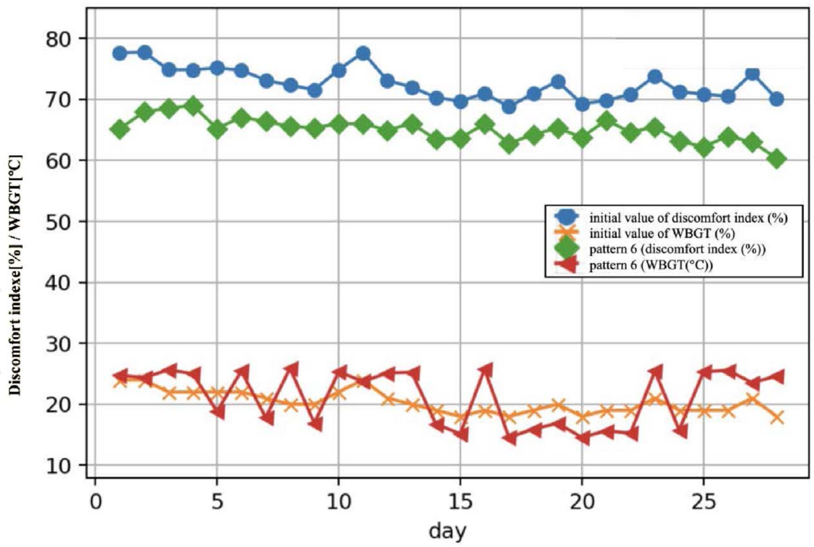

Figure 7. Results of Pattern 6 (October, Usable heat: 1,000,000 J).

characteristics, and calculation accuracy. The degree of influence from the weather forecast accuracy on the model was analyzed and verified.

The variance of the forecast error was adjusted for sensitivity analysis as shown in Equation (20):

$$\omega^2 = \alpha\sigma^2 \tag{20}$$

where,

ω^2: *adjusted* variance

σ^2: variance

α: parameter for sensibitiy analysis.

A simulation was conducted for July 2020. The DI target was 75, usable heat resource was 1,000,000 J, and alpha value was 0.1–5. The corresponding simulation results are shown in Figures 8–12. As the variance of the forecast error decreased, the peak value of the DI was controlled according to the tendency of its initial value and the low heat distribution. When the prediction accuracy deteriorated, variance also deteriorated significantly, and the heat resource was not distributed according

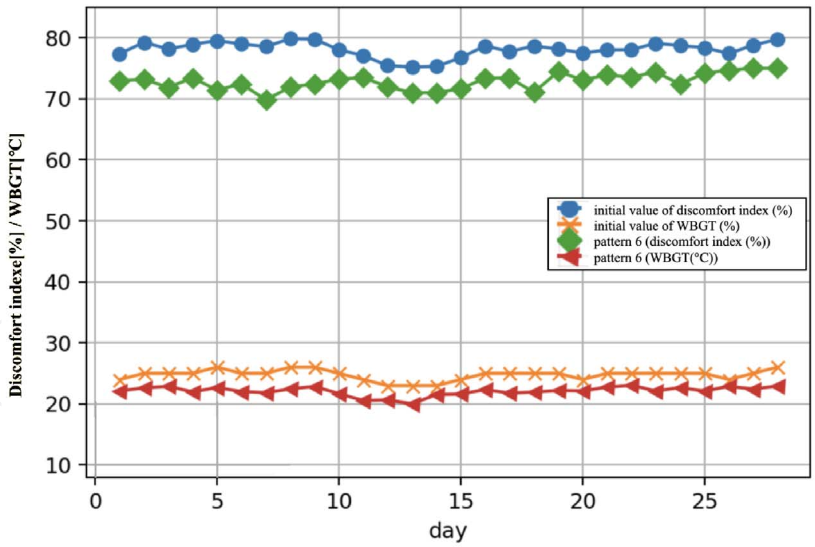

Figure 8. Simulations results when $\alpha = 1$.

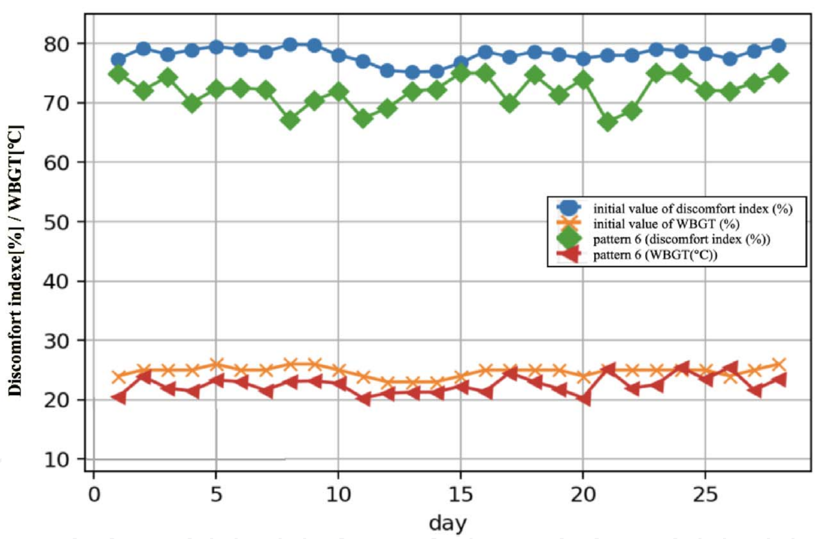

Figure 9. Simulation results when $\alpha = 2$.

to the weather forecast (Table 12). When the prediction accuracy was improved, a more stable heat distribution could be achieved. Figures 8–12 indicate that the room environment was not stable when the prediction accuracy deteriorated.

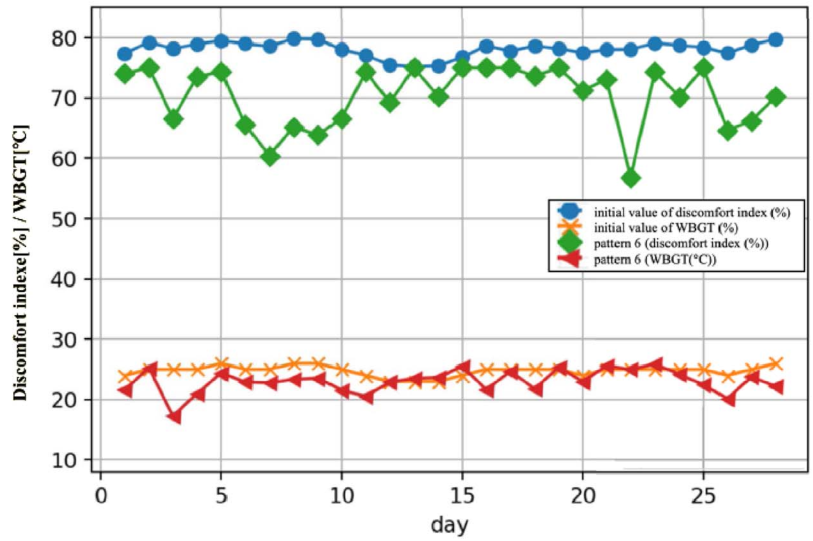

Figure 10. Simulation results when $\alpha = 5$.

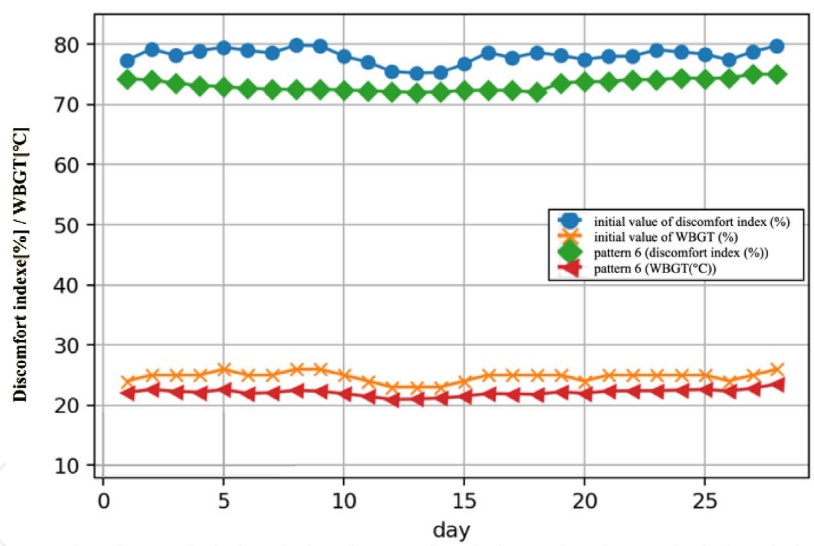

Figure 11. Simulation results when $\alpha = 0.5$.

Improvement in the prediction accuracy reflected the tendency of the initial value for the DI after several days, and by adjusting the peak value of the DI gradually, sudden changes in heat resource distribution can be avoided.

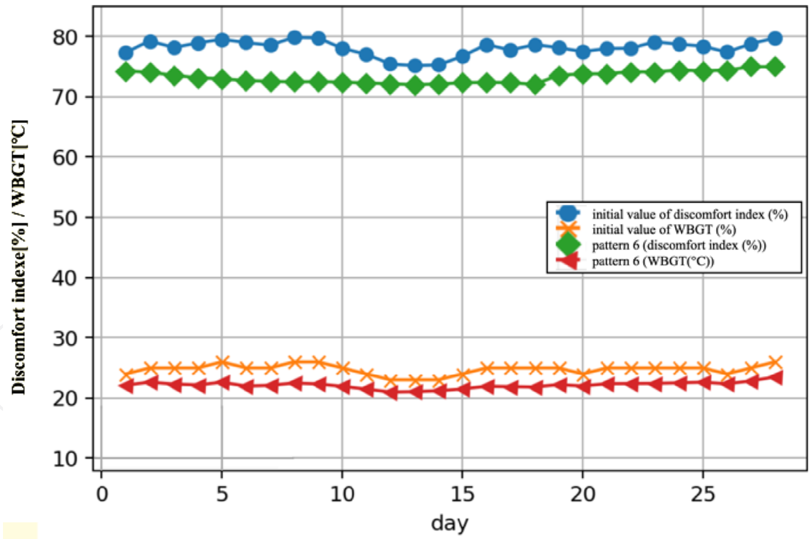

Figure 12. Simulation results when α = 0.1.

Table 12. Result of changing α (Average of 100 times).

	α = 1	α = 2	α = 5	α = 0.5	α = 0.1
Mean (July)	72.96	72.17	69.72	73.17	73.23
Variance (July)	2.01	5.86	26.99	1.18	0.91

5. Conclusions

In this study, we proposed a regression model to predict the initial value of the room environment using weather forecast data and a dynamic heat distribution model based on that forecast data. A dynamic air-conditioning operation planning model that could simulate conditions similar to the air-conditioning operation conditions, and comparatively verify each condition, was also proposed. Since these models are affected by weather forecast data, a sensitivity analysis was performed based on the accuracy of the weather forecast, and the subsequent effects were analyzed.

The results indicate that the target heat amount could be changed, considering the gap between the planned and actual heat utilization, and if the heat consumption exceeded the monthly target, the plan could be revised to use the heat resource for the next month in advance. On a broader scale, the proposed plan can assist facility managers in addressing problems such as daily changes in the thermal load and excessive use of target heat resources.

This study has a few limitations. Room characteristics affects the prediction of the initial conditions for the room environment. In this study, we assumed that the room environment changes depending only on weather conditions. However, other factors, such as mechanical heat, can also affect changes in the room environment. For example, if a heat-generating machine, with operating conditions changing daily, is installed in the room, the room environment is then significantly affected. Thus, additional factors should be considered in future studies.

Human-generated thermal load affects the heat consumption. However, considering the residents' dwell time and activity level for predicting thermal load in the medium to long term is not realistic due to constant fluctuations. The same applies to the influence of air-conditioning equipment. When changes in residents' dwell time and activity level outweigh the effects of weather conditions, the difference between actual heat usage and allocated heat usage is recognized and integrated into the planning.

While room characteristics and air conditioning systems also influence heat consumption, this approach focuses solely on the disparity between planned and actual heat usage, making it applicable to various room setups and facilities.

Moreover, the weather forecast period was 10 days for this study, and the date and time of the weather forecast up to 10 days ahead was considered. If the cooling operation period is several months, then predictions using the weather forecast data could be conducted in units for several months. Additionally, if the forecast accuracy for each day is constant, then the amount of heat would be distributed with the same weight. However, since prediction accuracy for the distant future is considered slightly lower than that of the near future, the variance value of the forecast should be increased gradually, and the amount of heat should be distributed accordingly.

Nomenclature

BEMS	Building and energy management system
DI	Discomfort index
WBGT	Wet-bulb globe temperature
FCU	Fan coil unit
Wbt	Wet bulb temperature (°C)
Bbt	Black bulb temperature (°C)
Dbt	Dry bulb temperature (°C)
$D^{t'}$	Initial value of the discomfort index
a_i	Partial regression coefficient
x_1^t:	Maximum temperature
x_2^t:	Minimum temperature
x_3^t:	Precipitation probability
x_4^t:	Precipitation
x_5^t:	Lightning probability
x_6^t:	Wind speed

x_7^t: Sunshine rate

x_8^t Sunshine duration

x_9^t: Minimum humidity

t' Forecast time

t: Observation time

$W^{t'}$ Intial value of WBGT

b_k Partial regression coefficient

q_i predicted heat usage on the ith day (J)

u_{sc} Predicted heat usage at the start-up time operation (J)

u_c Predicted heat usage at continuous operation (J)

$u_{su,\,ps}\,(D_{s\,(i)}, D_p)$ Heat consumption required per hour during the start-up operation to change the DI from $D_{s\,(i)}$ to D_p (kJ/s)

T_{su} Start-up operation time (s)

$u_{c,\,ps}\,(D_{s\,(i)}, D_p)$ Heat consumption required per hour during the continuous operation, to change the DI from $D_{s\,(i)}$ to D_p (kJ/s)

t_s: Start time of the operation (hh:mm:ss)

t_e: End time of the operation (hh:mm:ss)

$D_{s\,(i)}$ Initial value of the DI on the ith day

D_p: Target peak value of the DI

$W_{s\,(i)}$ Initial value of WBGT on the ith day

W_p Target peak value of WBGT

Q_i Heat amount used on the ith day

L Usable heat amount (J)

p Prediction period

d Number of days remaining until the last day of the operation period (days)

$f^Q\,(D_{s\,(i)}, D_p)$ The amount of heat required to reduce the discomfort index from $D_{s\,(i)}$ to D_p (J)

$D_r\,(i)$ Simulated value of the DI on the ith day

$D_a\,(i)$ Actual value of the DI on the ith day

ε Forecast error

ω^2 *adjusted* variance

σ^2 variance

α parameter for sensibitiy analysis.

Conflict of interest

The authors declare no conflict of interest.

References

1 Tazaki S. An overview of building control technology. *Trans Soc Heat Air Cond Sanit Eng Jpn*. 2008;**86**: 135–141.

2 Yuan J, Farnham C, Emura K. Development and application of a simple BEMS to measure energy consumption of buildings. *Energy Build*. 2015;**109**: 1–11. doi:https://doi.org/10.1016/J.ENBUILD.2015.10.012.

3 Rotger-Griful S, Welling U, Jacobsen R. Implementation of a building energy management system for residential demand response. *Microprocess Microsyst*. 2017;**55**: 100–110. doi:https://doi.org/10.1016/j.micpro.2017.10.006.

4 Karim MA, Hasan M, Khan MIH. A simplistic and efficient method of estimating air-conditioning load of commercial buildings in the sub-tropical climate. *Energy Build*. 2019;**203**: 109396. doi:https://doi.org/10.1016/j.enbuild.2019.109396.

5 Tanaka Y, Gondo T, Inoue T, Matsuo Y. Data analysis and prediction method of energy consumption in buildings. Part 1. Relations between energy consumption and weather factors. *Trans Soc Heat Air Cond Sanit Eng Jpn*. 1996;**21**: 123–131.

6 Agarwal Y, Weng T, Gupta RK. The energy dashboard: improving the visibility of energy consumption at a campus-wide scale. In: *Proceedings of the First ACM Workshop on Embedded Sensing Systems for Energy-Efficiency in Buildings*. New York: Association for Computing Machinery; 2009. p. 55–60. doi:https://doi.org/10.1145/1810279.1810292.

7 Rice A, Hay S, Ryder-Cook D. Limited-data model of building energy consumption. In: *Proceedings of 2nd ACM Workshop on Embedded Sensing Systems for Energy-Efficiency in Buildings*. New York: Association for Computing Machinery; 2010. p. 67–72. doi:https://doi.org/10.1145/1878431.1878447.

8 Zheng M, Nishitani Y, Nakahara N. Study on load prediction method based on Kalman filter. *Trans Soc Heat Air Cond Sanit Eng Jpn*. 1999;**24**(72):85–93. doi:https://doi.org/10.18948/shase.24.72_85.

9 Ikawa S, Kuramoto K, Kumagai S, Kishima S. Regression model for estimating thermal resource usage in air conditioning systems: daily demand forecast by potential integral method, considering thermal inertia of room and weather conditions. *Asian J Manage Sci Applicat*. 2019;**4**: 3–14. doi:http://dx.doi.org/10.1504/AJMSA.2019.10022887.

10 Kawashima M, Ito N. Sudy on real-time load prediction method for hvac system control. *J Archit Plan (Trans AIJ)*. 1996;**61**(484):43–51. doi:https://doi.org/10.3130/aija.61.43_3.

11 Nakamura Y, Kuriyama K, Yamamoto M, Asano Y. Optimum control of heating and cooling plant with thermal storage tanks. *Trans Soc Heat Air Cond Sanit Eng Jpn*. 2003;**90**: 121–131.

12 Yamaguchi H, Yoshida H. Development of optimum operation schemes for HVAC systems with a thermal storage tank considering the dehumidification performance. *Trans Soc Heat Air Cond Sanit Eng Jpn*. 2010;**159**: 19–25.

13 Yamaguchi H, Yoshida H, Matsushita N, Kitora H. Verification of optimum operation method by simulation for the HVAC system with a thermal storage tank in an actual building. *Trans Soc Heat Air Cond Sanit Eng Jpn*. 2011;**167**: 21–29.

14 Wang F, Zhou L, Ren H, Liu X, Talari S, Shafie-khah M, et al. Multi-objective optimization model of Source–Load–Storage synergetic dispatch for a building energy management system based on TOU price demand response. *IEEE Trans IA*. 2018;**54**: 1017–1028. doi:https://doi.org/10.1109/TIA.2017.2781639.

15 Kumagai S, Nakano W, Kishima S. Heat resource allocation algorithm for client-driven air conditioning in building energy management: formulation by 0-1 integer programming. *IEEJ Trans IA*. 2014;**134**: 505–516. doi:https://doi.org/10.1541/IEEJIAS.134.505.

16 Kumagai S, Kishima S. Building air conditioning model using the room-specific thermal inertia and its implementation as a controller: control method with the learning mechanism of thermal inertia in the building air conditioning. *IEEJ Trans Electron Inf Syst*. 2014;**134**: 620–633. doi:http://dx.doi.org/10.1541/ieejeiss.134.620.

17 Aizawa R, Kumagai S, Kishima S. Operation plan of air conditioning by saving and relocating heat resource to the virtual heat resource storage: estimation of room's heat inertia and heat resource allocation algorithm. *IEEJ Trans Electron Inf Syst*. 2015;**136**: 233–243. doi:https://doi.org/10.1541/IEEJEISS.136.233.

18 Dhar A, Reddy TA, Claridge D. A Fourier series model to predict hourly heating and cooling energy use in commercial buildings with outdoor temperature as the only weather variable. *J Sol Energy Eng*. 1999;**121**: 47–53. doi:http://dx.doi.org/10.1115/1.2888142.

19 Kinouchi T. A study on thermal indices for the outdoor environment. *Tenki*. 2001;**48**: 672–677.

20 Tanabe S. Evaluation of thermal comfort. *J Phys Soc Japan*. 1999;**54**: 440–448.